American Mineralogist, Volume 83, pages 775–785, 1998

# Crystal chemistry of Mg-, Fe-bearing muscovites-2$M_1$

MARIA FRANCA BRIGATTI,* PAOLA FRIGIERI, AND LUCIANO POPPI

Dipartimento di Scienze della Terra, Università di Modena, Modena, Italy

## ABSTRACT

Phengitic muscovite-2$M_1$ crystals $[^{[12]}(K_{0.88-0.99}Na_{0.01-0.09}Ca_{0.00-0.06}Ba_{0.00-0.01})^{[6]}(Al_{1.64-1.88}Fe^{2+}_{0.06-0.29}Fe^{3+}_{0.01-0.16}Mg_{0.00-0.16}Mn_{0.00-0.07}Ti_{0.00-0.06})^{[4]}(Si_{2.87-3.30}Al_{0.70-1.13})(OH)_{1.56-2.07}F_{0.00-0.41}O_{9.91-10.25}]$ from pegmatites and peraluminous granites were refined to investigate the influence of phengitic substitution on the mica structure. Single-crystal X-ray diffraction data were collected for eleven crystals in the *C2/c* space-group (agreement factor $2.1\% \leq R_{obs} \leq 3.9\%$). Tetrahedral Si and Al cation disorder was found for each sample, with the mean tetrahedral cation-oxygen distances ranging from $1.639\ \text{Å} \leq \langle T1\text{-}O \rangle \leq 1.647\ \text{Å}$ and $1.640\ \text{Å} \leq \langle T2\text{-}O \rangle \leq 1.646\ \text{Å}$. As phengitic substitution increases, the octahedral sheet expands and requires a less distorted (more hexagonal) tetrahedral ring ($7.70° \leq \alpha \leq 11.38°$) and low corrugation of the basal O plane ($0.1796\ \text{Å} \leq \Delta z \leq 0.2296\ \text{Å}$). The electron density at the M2 site is greater than that required for the ideal muscovite-2$M_1$ structure, and a small excess of electron density is found in the M1 site. The inner sixfold coordination of the interlayer (A) cation is elongated along **c***, which is consistent with the high $\alpha$ values and the long A-O11 bond length.

## INTRODUCTION

Dioctahedral true micas are common rock-forming minerals. Their compositions, though limited in comparison with the trioctahedral subgroup, cover a wide range of tetrahedral, octahedral, and interlayer populations.

The replacement of octahedral $Al^{3+}$ by $Fe^{2+}$, $Mg^{2+}$, and $Ti^{4+}$ in end-member muscovite $[KAl_2Si_3AlO_{10}(OH)_2]$ requires heterovalent substitutions involving tetrahedral, octahedral, and probably anion sites. These substitutions, as well as the homovalent substitutions of $Al^{3+}$ for $Fe^{3+}$ and $K^+$ for $Na^+$ (Guidotti and Sassi 1976; Guidotti 1978; Guidotti et al. 1994a, 1994b), received attention as possible indicators of muscovite crystallization conditions, and, in the case of metamorphic rocks, of the reactions involving mica minerals (Sassi et al. 1994). The studies of Guidotti et al. (1989, 1992) addressed white mica compositions and unit-cell dimensions and helped to establish the relationships between geometrical features and chemical data to understand the petrogenetic processes during formation of igneous and metamorphic rocks.

Except for disordered sequences, the most common layer stacking consists of the 2$M_1$ polytype, although 1*M*, 3*T*, and 2$M_2$ stackings also have been reported (Bailey 1984). The muscovite structure was outlined first by Jackson and West (1930, 1933), and crystals with variable phengitic content have since been investigated: refinements were performed for 2$M_1$ (Radoslovich 1960; Birle and Tettenhorst 1968; Güven 1971; Rothbauer 1971; Richardson and Richardson 1982), 1*M* (Sidorenko et al. 1977; Tsipurskii and Drits 1977), 3*T* (Güven and Burnham 1967; Amisano-Canesi et al. 1994; Pavese et al. 1997), and 2$M_2$ polytypes (Zhoukhlistov et al. 1973).

The first single-crystal X-ray structure determination of muscovite-2$M_1$ in the *C2/c* space group (R = 17%) found differences between the mean bond length of the two tetrahedral sites. Based on this evidence, Radoslovich (1960) proposed the ordering of Si and Al. Using the data of Radoslovich, Birle and Tettenhorst (1968) improved the accuracy of the refinement and found that coordination polyhedra were more regular than originally determined. However, the differences were not sufficiently large to indicate ordering of tetrahedral Al.

A single-crystal X-ray diffraction (XRD) study on a muscovite- and a phengite-2$M_1$ by Güven (1971) showed that tetrahedral Si and Al cations were disordered in the case of muscovite, whereas small differences between tetrahedral cation-oxygen distances in phengite were interpreted to indicate a very slight amount of tetrahedral ordering. Electron density was found in the "vacant" octahedral site in phengite (0.25 e/Å$^3$) and muscovite (0.4 e/Å$^3$). The tetrahedral rotation angle ($\alpha$) and the corrugation of the basal-oxygen surfaces ($\Delta z$) in muscovite were found to be about twice those in phengite.

In a neutron diffraction single-crystal determination of muscovite-2$M_1$ ($R$ = 2.7%), Rothbauer (1971) showed disordered tetrahedral Si and Al cation sites and protons located at a distance of 0.928(5) Å from O. He also showed that the O-H vector pointed toward the vacant site and was inclined at an angle ($\rho$) of +12° above the (001) plane. High values of tetrahedral out-of-plane tilting ($\Delta z$ = 0.213 Å) and tetrahedral rotation angle ($\alpha$ = 11°40′) were also found.

* E-mail: brigatti@unimo.it

0003–004X/98/0708–0775$05.00

**TABLE 1.** Dimensions, unit-cell parameters, and details of the structure refinements of muscovite-2$M_1$ crystals

| Samples | Dimensions (mm) | $N_{obs}$ | $R_{sym}$ ×100 | $R_{obs}$ ×100 | $a$ (Å) | $b$ (Å) | $c$ (Å) | β (°) | Vol (Å³) |
|---|---|---|---|---|---|---|---|---|---|
| GA1 | 0.50 × 0.40 × 0.02 | 1149 | 2.70 | 2.54 | 5.226(1) | 9.074(2) | 20.039(2) | 95.74(1) | 945.4(2) |
| RA1 | 1.20 × 0.90 × 0.02 | 1292 | 2.78 | 2.96 | 5.182(3) | 8.982(5) | 20.002(5) | 95.72(2) | 926(3) |
| A4b | 0.70 × 0.40 × 0.03 | 1222 | 2.80 | 3.58 | 5.186(1) | 8.991(3) | 20.029(7) | 95.77(3) | 929.1(4) |
| GFS15Ab | 0.24 × 0.15 × 0.02 | 1035 | 2.69 | 2.92 | 5.192(2) | 9.013(5) | 20.056(7) | 95.83(3) | 933(2) |
| H87b | 0.24 × 0.22 × 0.06 | 738 | 2.84 | 3.93 | 5.209(3) | 9.035(6) | 20.066(9) | 95.68(3) | 939.8(5) |
| CC1b | 0.50 × 0.30 × 0.01 | 1431 | 3.05 | 2.89 | 5.186(1) | 9.005(1) | 20.031(3) | 95.78(1) | 930.6(2) |
| C3-29b | 0.24 × 0.16 × 0.02 | 1174 | 3.11 | 2.78 | 5.188(1) | 8.996(3) | 20.082(2) | 95.78(1) | 932.5(3) |
| B1b | 0.40 × 0.20 × 0.02 | 1338 | 2.08 | 2.11 | 5.187(2) | 9.004(2) | 20.036(2) | 95.73(2) | 931.1(3) |
| C6Cb | 0.50 × 0.50 × 0.09 | 1302 | 2.54 | 3.87 | 5.186(1) | 9.003(1) | 20.030(4) | 95.84(2) | 930.3(3) |
| C6Bb | 0.50 × 0.44 × 0.02 | 1153 | 3.50 | 3.12 | 5.196(2) | 8.997(3) | 20.034(4) | 95.80(2) | 931.7(5) |
| C3-31b | 0.12 × 0.12 × 0.02 | 1007 | 2.56 | 2.80 | 5.197(1) | 9.022(2) | 20.076(4) | 95.79(2) | 936.6(4) |

*Note:* $R_{sym} = (\Sigma_{hkl} \Sigma_{i=1}^{N} |I_{(hkl)_i} - I_{(hkl)_i}|)/\Sigma_{hkl} \Sigma_{i=1}^{N} I_{(hkl)_i}$.

The crystal structure of a reversely pleochroic muscovite, containing both $Fe^{3+}$ and $Mn^{3+}$, was determined by Richardson and Richardson (1982) using single-crystal X-ray methods. They found that octahedrally coordinated sites were distorted, similar to the results of the neutron diffraction study (Rothbauer 1971) and, despite the unusual composition of this muscovite, no electron density excess was found in M1.

A chromian phengite structure (Rule and Bailey 1985) showed mean atomic number (m.a.n.) equal to 1.5 $e^-$ at the typically vacant M1 octahedral site, indicating partial occupancy. The H was located at 0.920 Å from the associated O within M1 ($\rho = -3.91°$). No ordering of tetrahedral cations was found, and the α (7.93°) and $\Delta z$ (0.184 Å) values were lower than in muscovite. Presumably, the substitution of Si for Al causes the tetrahedral sheet to become thinner and laterally smaller, so that less tetrahedral rotation is required. Consequently, the interlayer cation lies deeper in the larger opening of the tetrahedral ring. As the phengitic component increases, the typically vacant M1 site shrinks and the M2 site expands but distortions at both sites decrease. Thus, as the layers become more phengitic, the tetrahedral rotation and octahedral flattening become smaller and the lateral misfit decreases.

To investigate the effect of Mn substitution on muscovite-2$M_1$, Knurr and Bailey (1986) studied a Mn-bearing muscovite (alurgite). The H was located at a distance of 0.92 Å from the associated O and pointed toward M1. The mean T-O bond length for the T1 and T2 sites indicated tetrahedral Si and Al disorder. The increase in cell dimensions, mean <M2-O> bond length, and octahedral thickness are caused by the slight octahedral substitution of Mn, Fe, Mg, and Ti for Al, coupled with the phengitic enrichment in Si in tetrahedral sites.

Two muscovite-2$M_1$ crystals with different compositions, one very close to the ideal end-member (Panasqueira) and the other more phengitic (Keystone), were studied by Guggenheim et al. (1987). The refinement of the Panasqueira crystal showed that about one-half of an electron was present in the normally vacant M1 site, whereas the Keystone crystal refinement did not show any electron density at M1. A small substitution of $Fe^{2+}$, $Mn^{2+}$, or Na appeared to produce an increase in the $a$ and $b$ axial lengths. These substitutions also caused the corrugation of the basal-oxygen surface and the tetrahedral rotation angle to increase ($\Delta z$ = 0.209 Å; 0.213 Å and α = 11.3°; 11.8° for Keystone and Panasqueira, respectively).

In a study of muscovite-2$M_1$ by Catti et al. (1989), cation disorder between T1 and T2 was observed and the α value was 11.77°. The O-H vector was parallel to the (001) plane. Catti et al. (1994) investigated a 2$M_1$-muscovite (with high phengitic content) using powder neutron diffraction. The Rietveld refinement ($R$ = 4.0%) included the H atom position, and the refined scattering lengths of T1 and T2 supported Si and Al disorder. The tetrahedra were distorted whereas the α value of 7.9° was smaller than previously found for phengites. Two muscovite-2$M_1$ crystals, with different Na contents and very low phengitic substitution (Comodi and Zanazzi 1995), both showed an electron density excess in M1. For one crystal, the H was located at 0.8 Å from the associated O.

This study considers 11 new crystal structure refinements of muscovite-2$M_1$ having different compositions, together with the structure constraints that control possible chemical variations.

## EXPERIMENTAL DETAILS

### Samples

Crystals examined occur in: (1) peraluminous granites from Northern Victoria Land, Antarctica (C6Bb, C3-29b, C6Cb, CC1b, B1b, and C3-31b) and from Sardinia, Italy (A4b, GFS15Ab, and H87b); and (2) pegmatites from Antarctica (RA1) and from Maddalena Island, Italy (GA1). To select samples for X-ray study, crystals found in polished thin sections were analyzed by wavelength-dispersive electron microprobe methods. Compared with the ideal muscovite composition, the samples chosen exhibit the following substitutions:

$$^{[6]}Al^{3+}_{-1}{}^{[4]}Al^{3+}_{-1}{}^{[6]}(Mg^{2+}, Fe^{2+})^{[4]}Si^{4+} \quad (1)$$

$$^{[6]}Al^{3+}_{-2}{}^{[6]}Ti^{4+}{}^{[6]}(Mg^{2+}, Fe^{2+}) \quad (2)$$

$$^{[6]}Ti^{4+}_{-1}{}^{[4]}Al^{3+}_{-1}{}^{[6]}AL^{3+}{}^{[4]}Si^{4+} \quad (3)$$

$$^{[6]}(Mg^{2+}, Mn^{2+}, Fe^{2+})_{-1}{}^{[4]}Si^{4+}_{-1}{}^{[6]}Ti^{4+}{}^{[4]}Al^{3+} \quad (4)$$

The exchange vector (Eq. 1) represents the phengitic substitution, whereas the sum of the (Eq. 1) and (Eq. 4) vectors is the celadonite substitution (Guidotti et al. 1989). Guidotti (1978, 1984) interpreted exchange vectors (Eq. 2) and (Eq. 3) as a response of the octahedral sheet to the introduction of Ti to preserve dioctahedral character.

To exclude zoning and interlayering of phases, crystals with **c*** parallel and normal to the electron beam were examined by scanning electron microscopy (Philips SEM XL 40 with energy dispersive detector and BeO window), by backscattered electron imaging and by X-ray maps.

### Single-crystal X-ray data collection and structure refinement

Crystals were selected from crushed rock fragments, examined by optical microscopy, and then studied by precession or Weissenberg photographs. Those crystals showing sharp reflections and minimal streaking for $k \neq 3n$ reflections were chosen for cell dimension and intensity data collection. Only 11 muscovite $2M_1$ crystals were suitable for further study.

Crystals from samples C6Bb, C3-29b, C6Cb, CC1b, B1b, C3-31b, A4b, H87b, and GA1 were mounted on a Siemens P4P rotating-anode single-crystal diffractometer with graphite-monochromatized Mo$K\alpha$ X radiation, operating at 50 kV and 140 mA, and equipped with XSCANS software (Siemens 1993). Crystals from samples GFS-15Ab and RA1 were studied with an automated CAD4 (Enraf-Nonius) four-circle diffractometer, using graphite-monochromatized Mo$K\alpha$ X radiation operating at 52 kV and 40 mA. Unit-cell parameters (Table 1) were determined by least-squares refinement of nearly 25 medium-high angle reflections.

Four octants of the reflection sphere were measured in the $2\theta$ range 4.0–65.0° using $\omega$ scan, window width from 1.4 to 5.8°, and variable reflection scanning speeds. The intensity and position of three standard reflections were checked every 100 reflections to monitor crystal and electronic stability. Absorption effects were corrected using a complete $\psi$ scan from 0 to 360° at 10° $\phi$ intervals, and Lorentz-polarization effects were determined. The symmetrically equivalent reflection intensities were averaged and the resulting discrepancy factors ($R_{sym}$) were calculated (Table 1). Statistical tests and crystal structure refinement in the $C2$ and $Cc$ subgroups were performed on the complete set of intensity data to verify that the unit cells were centrosymmetric. No significant symmetry lowering was detected, and the $C2/c$ space group was therefore chosen for all crystals. The crystal structure refinements were performed using the ORFLS least-squares program (Busing et al. 1962). No weights and no constraints were used during the refinement; a reflection was considered as observed if $F_{obs} \geq 5\sigma_{F_{obs}}$ (Ungaretti 1980; Ungaretti et al. 1983).

Atomic position parameters from Guggenheim et al. (1987) were used as initial values. Fully ionized scattering factors were used for the M2 octahedral and A interlayer sites, whereas mixed scattering factors were assumed for the anion (O vs. $O^{2-}$) and tetrahedral sites (75Si-25Al vs. $75Si^{4+}$-$25Al^{3+}$). During the last anisotropic cycle of the refinement, curves appropriate for the chemical composition of each crystal were introduced and a complete Fourier difference electron density (DED) map was calculated. The DED map showed the presence of an electron density excess in the "vacant" M1 position for all crystals; the introduction of the M1 site in the refinement significantly improved the agreement index ($R_{obs}$). Several cycles of anisotropic refinement converged to final $R_{obs}$ values, ranging from 2.1 to 3.9%. A careful examination of the final DED map of crystals GA1, GFS15Ab, CC1b, C3-29b, B1b, C6Bb, and C3-31b revealed an electron density excess above background ($>3\sigma$) close to the H position [$x/a$ = 0.8727(7), $y/b$ = 0.1499(4), $z/c$ = 0.0599(2)] suggested by the Rothbauer (1971) neutron diffraction structural refinement (GA1: $x/a$ = 0.876, $y/b$ = 0.143, $z/c$ = 0.046; GFS15Ab: $x/a$ = 0.872, $y/b$ = 0.153, $z/c$ = 0.055; CC1b: $x/a$ = 0.891, $y/$

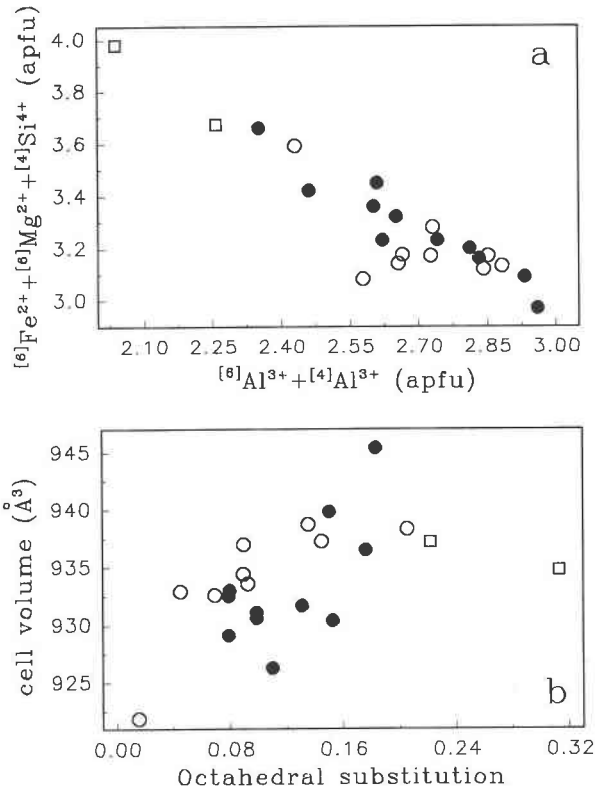


**FIGURE 1.** (**a**) $^{[6]}Fe^{2+}$ + $^{[6]}Mg^{2+}$ + $^{[4]}Si^{4+}$ apfu vs. $^{[6]}Al$ + $^{[4]}Al$ apfu (phengitic exchange vector); and (**b**) Cell volume (Å$^3$) vs. octahedral substitution calculated as ($Fe^{2+}$ + $Fe^{3+}$ + $Mg^{2+}$ + $Ti^{4+}$ + $Mn^{2+}$)/($Fe^{2+}$ + $Fe^{3+}$ + $Mg^{2+}$ + $Ti^{4+}$ + $Mn^{2+}$ + $^{[6]}Al^{3+}$) of muscovite-$2M_1$ crystals. Symbols: filled circles = samples from this study; open circles = muscovite samples from the literature (Birle and Tettenhorst 1968; Güven 1971; Rothbauer 1971; Richardson and Richardson 1982; Knurr and Bailey 1986; Guggenheim et al. 1987; Catti et al. 1989, 1994); open squares = phengites from literature (Güven 1971; Rule and Bailey 1985).

**Table 2.** Crystallographic coordinates and equivalent isotropic (Å$^2$) and anisotropic temperature factors (Å$^2$ × 10$^4$) of muscovite-2$M_1$ crystals

| Atom | x/a | y/b | z/c | $B_{eq}$ | $\beta_{11}$* | $\beta_{22}$* | $\beta_{33}$* | $\beta_{12}$* | $\beta_{13}$* | $\beta_{23}$* |
|---|---|---|---|---|---|---|---|---|---|---|
| | | | | | **GA1** | | | | | |
| O11 | 0.7402(3) | 0.3211(2) | 0.15966(8) | 1.44(4) | 96(6) | 57(2) | 8.4(4) | −27(3) | −2(1) | 3.3(7) |
| O21 | 0.2410(3) | 0.3611(2) | 0.16867(8) | 1.35(4) | 105(6) | 52(2) | 7.2(4) | 31(3) | 1(1) | −0.9(7) |
| O22 | 0.4344(3) | 0.0927(2) | 0.16815(8) | 1.31(3) | 161(6) | 28(2) | 7.4(3) | 6(3) | 1(1) | 0.1(7) |
| O31 | 0.3924(3) | 0.2514(2) | 0.05367(7) | 1.04(3) | 94(5) | 41(2) | 4.4(3) | 3(3) | 0.8(9) | 2.3(6) |
| O32 | 0.9572(3) | 0.4398(2) | 0.05377(7) | 1.09(3) | 106(5) | 41(2) | 4.6(3) | −2(2) | 1(1) | 1.2(6) |
| O4 | 0.9549(3) | 0.0646(2) | 0.05098(8) | 1.24(3) | 149(6) | 40(2) | 4.9(3) | 19(3) | 4(1) | −2.4(6) |
| A | 0 | 0.0962(1) | 0.25 | 1.86(2) | 160(2) | 60.6(8) | 11.4(2) | 0 | 2.4(5) | 0 |
| T1 | 0.4527(1) | 0.25782(6) | 0.13538(3) | 0.58(1) | 42(2) | 18.6(5) | 3.9(1) | 3.0(9) | −0.5(3) | 0.3(2) |
| T2 | 0.9642(1) | 0.42858(6) | 0.13538(3) | 0.56(1) | 47(2) | 15.9(6) | 3.7(1) | 0.0(8) | 0.6(3) | 0.7(2) |
| M2 | 0.2497(1) | 0.08323(6) | 0.00002(3) | 0.68(1) | 56(1) | 21.8(5) | 4.7(1) | 0.9(8) | 0.4(3) | 0.9(2) |
| M1 | 0.75 | 0.25 | 0 | 0.73 | | | | | | |
| | | | | | **RA1** | | | | | |
| O11 | 0.7502(3) | 0.3103(2) | 0.15785(9) | 1.69(4) | 122(5) | 43(2) | 14.8(4) | −22(2) | 1(1) | 4.7(7) |
| O21 | 0.2495(3) | 0.3700(2) | 0.16908(8) | 1.64(4) | 128(5) | 48(2) | 12.3(4) | 11(2) | 0(1) | −0.8(7) |
| O22 | 0.4170(3) | 0.0935(2) | 0.16837(8) | 1.70(3) | 162(5) | 34(2) | 14.4(4) | −10(3) | 8(1) | 0.7(7) |
| O31 | 0.3851(3) | 0.2519(2) | 0.05348(8) | 1.42(3) | 94(4) | 41(2) | 12.0(4) | −1(2) | 2(1) | 0.9(7) |
| O32 | 0.9622(3) | 0.4443(2) | 0.05363(8) | 1.41(3) | 101(5) | 37(2) | 12.2(4) | 3(2) | 1(1) | 0.9(6) |
| O4 | 0.9569(3) | 0.0617(2) | 0.05025(8) | 1.33(3) | 75(4) | 33(2) | 13.4(4) | −8(2) | 6(1) | −1.8(6) |
| A | 0 | 0.0982(1) | 0.25 | 2.39(2) | 203(3) | 73(1) | 16.6(2) | 0 | 4.5(6) | 0 |
| T1 | 0.4513(1) | 0.25857(7) | 0.13560(3) | 1.15(1) | 76(2) | 29.9(6) | 10.5(1) | −2.3(9) | 1.6(4) | 0.0(3) |
| T2 | 0.9649(1) | 0.42962(6) | 0.13554(3) | 1.09(1) | 74(2) | 22.3(6) | 11.0(1) | 0.6(8) | 2.8(3) | 0.1(2) |
| M2 | 0.2496(1) | 0.08332(7) | 0.00005(3) | 1.26(1) | 89(2) | 32.2(6) | 11.2(1) | −2.5(9) | 1.8(3) | 0.7(2) |
| M1 | 0.75 | 0.25 | 0 | 2.00 | | | | | | |
| | | | | | **A4b** | | | | | |
| O11 | 0.7512(4) | 0.3110(2) | 0.1578(1) | 1.67(4) | 108(6) | 52(2) | 13.7(5) | −14(3) | 3(1) | 3.1(9) |
| O21 | 0.2506(4) | 0.3703(2) | 0.1690(1) | 1.60(4) | 113(6) | 56(3) | 11.4(4) | 18(3) | 6(1) | −0.1(8) |
| O22 | 0.4184(4) | 0.0936(2) | 0.16844(9) | 1.58(4) | 126(6) | 46(2) | 12.3(4) | −7(3) | 8(1) | 0.1(8) |
| O31 | 0.3864(3) | 0.2510(2) | 0.05367(9) | 1.12(3) | 62(5) | 35(2) | 10.0(4) | 5(3) | 2(1) | 1.1(7) |
| O32 | 0.9618(3) | 0.4434(2) | 0.05378(9) | 1.18(4) | 83(5) | 37(2) | 9.3(4) | 12(3) | 4(1) | 0.2(7) |
| O4 | 0.9576(3) | 0.0622(2) | 0.05022(9) | 1.33(4) | 111(6) | 36(2) | 10.5(4) | 1(3) | 8(1) | −1.1(7) |
| A | 0 | 0.0988(1) | 0.25 | 2.22(2) | 181(3) | 70(1) | 15.9(2) | 0 | 7.7(6) | 0 |
| T1 | 0.4511(1) | 0.25862(8) | 0.13549(3) | 1.03(1) | 70(2) | 29.0(8) | 8.9(2) | 4(1) | 3.1(4) | 0.6(3) |
| T2 | 0.9649(1) | 0.43006(8) | 0.13547(4) | 1.01(1) | 66(2) | 28.0(8) | 9.1(2) | 1(1) | 4.1(4) | 0.7(3) |
| M2 | 0.2500(1) | 0.08358(8) | −0.00001(4) | 1.02(1) | 69(2) | 27.8(8) | 9.0(1) | −0(1) | 3.7(4) | 1.0(3) |
| M1 | 0.75 | 0.25 | 0 | 2.00 | | | | | | |
| | | | | | **GFS15Ab** | | | | | |
| O11 | 0.7499(4) | 0.3109(2) | 0.1574(1) | 1.79(5) | 126(7) | 66(2) | 12.0(5) | −26(4) | 6(1) | 5.3(9) |
| O21 | 0.2485(4) | 0.3701(2) | 0.1686(1) | 1.73(5) | 171(8) | 54(2) | 10.2(5) | 13(3) | 5(2) | −1.4(9) |
| O22 | 0.4171(4) | 0.0935(2) | 0.1681(1) | 1.70(4) | 183(7) | 45(2) | 10.8(5) | 0(4) | 10(1) | 0.5(9) |
| O31 | 0.3841(4) | 0.2513(2) | 0.05340(9) | 1.45(4) | 141(7) | 45(2) | 8.8(4) | 2(3) | 5(1) | −0.2(9) |
| O32 | 0.9610(4) | 0.4432(2) | 0.05337(9) | 1.32(4) | 121(7) | 38(2) | 9.1(4) | 4(3) | 6(1) | 0.8(8) |
| O4 | 0.9557(4) | 0.0620(2) | 0.05007(9) | 1.51(4) | 129(7) | 48(2) | 10.5(5) | −10(3) | 10(1) | −1.9(8) |
| A | 0 | 0.0986(1) | 0.25 | 2.23(2) | 213(4) | 66(1) | 14.5(2) | 0 | 8.7(7) | 0 |
| T1 | 0.4517(1) | 0.25880(8) | 0.13549(4) | 1.15(1) | 84(2) | 35.1(8) | 9.1(2) | 0(1) | 6.7(5) | 0.3(3) |
| T2 | 0.9648(1) | 0.42995(8) | 0.13538(4) | 1.09(1) | 89(2) | 28.0(7) | 9.2(2) | −3(1) | 8.2(5) | 0.3(3) |
| M2 | 0.2499(2) | 0.08307(9) | 0.00004(4) | 1.25(1) | 102(2) | 37.5(8) | 9.3(2) | −7(1) | 7.2(5) | 0.2(3) |
| M1 | 0.75 | 0.25 | 0 | 2.5(7) | | | | | | |
| | | | | | **H87b** | | | | | |
| O11 | 0.7472(8) | 0.3137(4) | 0.1584(2) | 2.5(1) | 202(20) | 78(5) | 17.1(8) | −12(8) | 6(3) | 6(2) |
| O21 | 0.2437(8) | 0.3674(4) | 0.1692(2) | 2.6(1) | 247(22) | 84(5) | 14.4(8) | 7(8) | 4(3) | −3(1) |
| O22 | 0.4230(7) | 0.0929(4) | 0.1684(1) | 2.22(9) | 196(20) | 64(4) | 15.3(7) | 0(8) | 8(3) | −1(1) |
| O31 | 0.3903(7) | 0.2516(4) | 0.0537(1) | 2.09(9) | 185(19) | 69(4) | 12.9(7) | 13(8) | 10(2) | 3(1) |
| O32 | 0.9620(8) | 0.4421(4) | 0.0536(1) | 2.10(9) | 185(20) | 71(4) | 12.3(7) | −4(7) | 8(3) | 2(1) |
| O4 | 0.9555(8) | 0.0636(4) | 0.0504(1) | 2.1(1) | 180(20) | 67(4) | 13.8(7) | −5(7) | 12(3) | −3(1) |
| A | 0 | 0.0979(2) | 0.25 | 2.99(5) | 249(10) | 93(2) | 20.6(4) | 0 | 12(1) | 0 |
| T1 | 0.4520(3) | 0.2578(2) | 0.13565(6) | 1.69(4) | 114(8) | 56(2) | 12.5(3) | 1(3) | 7.2(9) | 0.0(5) |
| T2 | 0.9647(3) | 0.4289(1) | 0.13567(6) | 1.73(4) | 146(8) | 51(2) | 12.2(3) | −1(3) | 8(1) | 1.0(5) |
| M2 | 0.2507(3) | 0.0835(1) | 0.00009(6) | 1.86(3) | 136(6) | 61(1) | 13.5(2) | 2(3) | 8.1(8) | 0.9(5) |
| M1 | 0.75 | 0.25 | 0 | 1.0(4) | | | | | | |
| | | | | | **CC1b** | | | | | |
| O11 | 0.7503(3) | 0.3114(2) | 0.15768(7) | 1.24(3) | 96(4) | 42(2) | 8.0(3) | −18(2) | −1.0(9) | 5.3(6) |
| O21 | 0.2494(3) | 0.3698(2) | 0.16880(7) | 1.08(3) | 84(4) | 36(2) | 7.3(3) | 16(2) | 1.5(9) | −2.7(5) |
| O22 | 0.4180(3) | 0.0930(2) | 0.16826(7) | 1.06(3) | 138(5) | 23(1) | 6.3(3) | 5(2) | 6.7(9) | 0.1(5) |
| O31 | 0.3854(2) | 0.2513(1) | 0.05351(6) | 0.69(2) | 73(4) | 19(1) | 4.4(2) | −4(2) | 3.7(8) | 0.5(4) |
| O32 | 0.9613(2) | 0.4433(1) | 0.05344(6) | 0.71(2) | 60(4) | 21(1) | 5.1(3) | 4(2) | 3.4(8) | 0.4(5) |
| O4 | 0.9572(2) | 0.0619(1) | 0.05034(6) | 0.79(2) | 68(4) | 24(1) | 5.7(3) | −5(2) | 6.0(8) | −2.6(5) |
| A | 0 | 0.09858(8) | 0.25 | 1.74(1) | 164(2) | 53.7(7) | 10.9(1) | 0 | 5.5(4) | 0 |
| T1 | 0.45162(9) | 0.25835(5) | 0.13548(2) | 0.50(1) | 36(1) | 13.3(5) | 4.3(1) | −0.4(7) | 1.8(3) | 0.3(2) |
| T2 | 0.96505(9) | 0.42957(5) | 0.13546(2) | 0.48(1) | 38(1) | 11.5(5) | 4.3(1) | 0.4(6) | 2.6(3) | 0.4(2) |
| M2 | 0.2491(1) | 0.08314(6) | 0.00002(3) | 0.58(1) | 44(1) | 15.9(5) | 4.8(1) | −1.6(7) | 2.3(3) | 0.5(2) |
| M1 | 0.75 | 0.25 | 0 | 0.8(4) | | | | | | |

**TABLE 2**—*Continued*

| Atom | x/a | y/b | z/c | $B_{eq}$ | $\beta_{11}$* | $\beta_{22}$* | $\beta_{33}$* | $\beta_{12}$* | $\beta_{13}$* | $\beta_{23}$* |
|---|---|---|---|---|---|---|---|---|---|---|
| | | | | | **C3-29b** | | | | | |
| O11 | 0.7513(3) | 0.3109(2) | 0.15723(8) | 1.35(4) | 101(6) | 50(2) | 8.3(4) | −18(3) | 0(1) | 3.7(7) |
| O21 | 0.2511(3) | 0.3705(2) | 0.16872(8) | 1.15(3) | 96(6) | 39(2) | 7.3(4) | 16(2) | 0(1) | −1.4(7) |
| O22 | 0.4168(3) | 0.0933(2) | 0.16823(8) | 1.16(3) | 136(6) | 30(2) | 6.8(3) | 6(3) | 8(1) | 0.5(7) |
| O31 | 0.3838(3) | 0.2514(2) | 0.05333(7) | 0.81(3) | 77(5) | 23(2) | 5.4(3) | 0(2) | 3(1) | 0.9(6) |
| O32 | 0.9614(3) | 0.4440(2) | 0.05332(7) | 0.79(3) | 55(5) | 30(2) | 5.2(3) | 5(2) | 4(1) | 1.0(6) |
| O4 | 0.9574(3) | 0.0617(2) | 0.05023(7) | 0.85(3) | 61(5) | 30(2) | 6.0(3) | 1(2) | 7(1) | −1.7(6) |
| A | 0 | 0.09898(9) | 0.25 | 1.78(2) | 168(3) | 57.2(9) | 10.8(2) | 0 | 6.4(5) | 0 |
| T1 | 0.4514(1) | 0.25854(6) | 0.13533(3) | 0.59(1) | 41(2) | 18.0(6) | 4.7(1) | 0.6(9) | 2.4(3) | 0.4(2) |
| T2 | 0.9653(1) | 0.42973(6) | 0.13533(3) | 0.57(1) | 44(2) | 16.0(6) | 4.7(1) | 1.0(8) | 3.9(3) | 0.5(2) |
| M2 | 0.2498(1) | 0.08332(7) | 0.00003(3) | 0.67(1) | 43(2) | 22.1(6) | 5.2(1) | 0.0(9) | 3.8(3) | 0.6(2) |
| M1 | 0.75 | 0.25 | 0 | 3.6(9) | | | | | | |
| | | | | | **B1b** | | | | | |
| O11 | 0.7490(2) | 0.3121(2) | 0.15786(6) | 1.26(3) | 108(4) | 47(2) | 6.7(3) | −18(2) | −0.3(8) | 5.1(5) |
| O21 | 0.2489(2) | 0.3692(1) | 0.16888(6) | 1.11(3) | 106(4) | 40(1) | 5.7(3) | 17(2) | 1.4(8) | −1.9(5) |
| O22 | 0.4193(2) | 0.0931(1) | 0.16832(6) | 1.15(3) | 155(4) | 27(1) | 5.9(3) | 6(2) | 6.3(8) | 0.2(5) |
| O31 | 0.3846(2) | 0.2517(1) | 0.05348(5) | 0.78(2) | 84(4) | 21(1) | 4.8(2) | 0(2) | 2.2(7) | 1.0(4) |
| O32 | 0.9613(2) | 0.4436(1) | 0.05350(5) | 0.78(2) | 71(4) | 25(1) | 4.8(2) | 4(2) | 1.9(7) | 0.9(4) |
| O4 | 0.9577(2) | 0.0618(1) | 0.05033(6) | 0.87(2) | 82(4) | 26(1) | 5.8(3) | −6(2) | 5.8(8) | −2.9(5) |
| A | 0 | 0.09854(7) | 0.25 | 1.78(1) | 177(2) | 55.8(7) | 10.3(1) | 0 | 3.8(4) | 0 |
| T1 | 0.45172(8) | 0.25839(5) | 0.13550(2) | 0.55(1) | 52(1) | 15.0(5) | 3.8(1) | 0.9(6) | 0.9(3) | 0.0(2) |
| T2 | 0.96512(8) | 0.42959(5) | 0.13547(2) | 0.56(1) | 55(1) | 14.7(5) | 3.8(1) | 0.0(6) | 2.1(3) | 0.6(2) |
| M2 | 0.24870(9) | 0.08287(5) | 0.00003(2) | 0.62(1) | 59(1) | 16.9(5) | 4.3(1) | 0.3(7) | 1.7(3) | 0.6(2) |
| M1 | 0.75 | 0.25 | 0 | 2.6(7) | | | | | | |
| | | | | | **C6Cb** | | | | | |
| O11 | 0.7502(4) | 0.3104(2) | 0.15748(8) | 1.63(4) | 194(7) | 54(2) | 6.3(3) | −21(3) | −4(1) | 6.4(6) |
| O21 | 0.2494(4) | 0.3700(2) | 0.16878(8) | 1.51(4) | 189(7) | 48(2) | 5.8(3) | 19(3) | −4(1) | −2.8(6) |
| O22 | 0.4173(4) | 0.0931(2) | 0.16831(8) | 1.44(4) | 226(7) | 32(2) | 5.6(3) | 4(3) | 4(1) | 0.4(6) |
| O31 | 0.3851(3) | 0.2515(2) | 0.05348(7) | 1.16(3) | 169(6) | 32(2) | 3.7(3) | 2(3) | −1(1) | 0.0(5) |
| O32 | 0.9612(3) | 0.4440(2) | 0.05342(7) | 1.13(3) | 148(6) | 37(2) | 3.7(3) | 2(3) | −1(1) | 1.4(5) |
| O4 | 0.9575(4) | 0.0618(2) | 0.05027(7) | 1.17(3) | 153(6) | 35(2) | 4.7(3) | −2(3) | 3(1) | −2.4(5) |
| A | 0 | 0.0986(1) | 0.25 | 2.13(2) | 267(4) | 65.4(9) | 8.8(2) | 0 | 1.5(6) | 0 |
| T1 | 0.4516(1) | 0.25846(6) | 0.13551(3) | 0.89(1) | 129(2) | 24.7(6) | 2.9(1) | 1(1) | −1.5(3) | 0.3(2) |
| T2 | 0.9650(1) | 0.42949(6) | 0.13546(3) | 0.89(1) | 131(2) | 23.9(6) | 2.9(1) | 0.9(9) | −0.5(3) | 0.8(2) |
| M2 | 0.2496(1) | 0.08311(7) | 0.00002(3) | 1.05(1) | 148(2) | 28.8(6) | 3.8(1) | −2(1) | −1.6(4) | 0.8(2) |
| M1 | 0.75 | 0.25 | 0 | 5.4(4) | | | | | | |
| | | | | | **C6Bb** | | | | | |
| O11 | 0.7501(3) | 0.3119(2) | 0.15770(9) | 1.67(4) | 115(6) | 57(2) | 12.1(4) | −8(3) | 2(1) | 4.0(8) |
| O21 | 0.2480(3) | 0.3700(2) | 0.16874(8) | 1.43(4) | 110(6) | 50(2) | 9.3(4) | 19(3) | 3(1) | −1.7(7) |
| O22 | 0.4183(3) | 0.0932(2) | 0.16835(8) | 1.51(4) | 149(6) | 47(2) | 9.0(4) | 2(3) | 4(1) | 0.2(7) |
| O31 | 0.3858(3) | 0.2517(2) | 0.05345(8) | 1.11(3) | 103(5) | 33(2) | 7.3(3) | 3(3) | 4(1) | 1.7(6) |
| O32 | 0.9607(3) | 0.4438(2) | 0.05349(8) | 1.09(3) | 83(5) | 37(2) | 7.7(4) | 0(2) | 5(1) | 0.6(6) |
| O4 | 0.9575(3) | 0.0619(2) | 0.05033(8) | 1.32(4) | 125(6) | 42(2) | 8.3(4) | −5(3) | 7(1) | −1.8(7) |
| A | 0 | 0.0988(1) | 0.25 | 2.08(2) | 194(3) | 67(1) | 12.8(2) | 0 | 5.8(6) | 0 |
| T1 | 0.4515(1) | 0.25858(7) | 0.13550(3) | 0.92(1) | 72(2) | 27.3(7) | 7.0(1) | 1(1) | 2.6(4) | 0.5(2) |
| T2 | 0.9652(1) | 0.42995(7) | 0.13539(3) | 0.90(1) | 73(2) | 25.0(7) | 7.1(1) | 0.9(9) | 3.9(4) | 0.3(2) |
| M2 | 0.2494(1) | 0.08322(7) | 0.00005(3) | 0.97(1) | 77(2) | 30.0(7) | 7.1(1) | −2(1) | 3.4(4) | 1.1(3) |
| M1 | 0.75 | 0.25 | 0 | 8(1) | | | | | | |
| | | | | | **C3-31b** | | | | | |
| O11 | 0.7491(4) | 0.3116(2) | 0.1578(1) | 1.25(4) | 88(6) | 45(2) | 8.3(5) | −13(3) | −1(1) | 4.1(8) |
| O21 | 0.2487(4) | 0.3696(2) | 0.16895(9) | 1.11(4) | 91(6) | 37(2) | 7.0(4) | 13(3) | −2(1) | −2.4(8) |
| O22 | 0.4190(4) | 0.0933(2) | 0.16840(9) | 1.10(4) | 132(6) | 28(2) | 6.3(4) | 1(3) | 4(1) | −0.2(8) |
| O31 | 0.3844(3) | 0.2518(2) | 0.05355(8) | 0.82(3) | 73(6) | 23(2) | 5.8(4) | 2(3) | 0(1) | 1.4(8) |
| O32 | 0.9612(3) | 0.4438(2) | 0.05345(8) | 0.74(4) | 57(6) | 24(2) | 5.1(4) | 0(3) | 1(1) | 0.3(7) |
| O4 | 0.9570(3) | 0.0619(2) | 0.05038(9) | 0.88(4) | 70(6) | 27(2) | 6.5(4) | −3(3) | 4(1) | −2.6(7) |
| A | 0 | 0.0985(1) | 0.25 | 1.75(2) | 162(3) | 55(1) | 10.8(2) | 0 | 4.4(6) | 0 |
| T1 | 0.4514(1) | 0.25841(7) | 0.13547(3) | 0.54(1) | 38(2) | 15.1(7) | 4.6(1) | 2(1) | 1.0(4) | 0.1(3) |
| T2 | 0.9650(1) | 0.42973(7) | 0.13537(3) | 0.54(1) | 41(2) | 14.6(7) | 4.4(1) | 0(1) | 1.8(4) | 0.3(3) |
| M2 | 0.2491(1) | 0.08314(7) | 0.00003(4) | 0.64(1) | 48(2) | 17.3(7) | 5.2(1) | 0(1) | 1.5(4) | 0.3(3) |
| M1 | 0.75 | 0.25 | 0 | 0.4(4) | | | | | | |

* Anisotropic temperature factors $\beta_{ij}$ are of the form $\exp[-(h^2\beta_{11} + \ldots + 2hk\beta_{12} + \ldots)]$.

$b$ = 0.130, $z/c$ = 0.060; C3-29b: $x/a$ = 0.870, $y/b$ = 0.145, $z/c$ = 0.062; B1b: $x/a$ = 0.873, $y/b$ = 0.147, $z/c$ = 0.060; C6Bb: $x/a$ = 0.885, $y/b$ = 0.165, $z/c$ = 0.062; C3-31b: $x/a$ = 0.894, $y/b$ = 0.135, $z/c$ = 0.069). In sample C6Cb, there is a peak (3σ above background) at $x/a$ = 0.961, $y/b$ = 0.098, $z/c$ = 0.106, whereas no reliable peaks were found for samples H87b, RA1, and A4b in the region where H could reasonably occur. In mosaic crystals, it is difficult to distinguish DED peaks that have physical meaning from those that are artifacts of errors (Nelson and Guggenheim 1993). Actually, electron density excess in close proximity to an O atom may be re-

**TABLE 3.** Selected bond lengths (Å) from structure refinements of muscovite-2$M_1$ crystals

| | GA1 | RA1 | A4b | GFS15A | H87b | CC1b | C3-29b | B1b | C6Cb | C6Bb | C3-31b |
|---|---|---|---|---|---|---|---|---|---|---|---|
| **Tetrahedral bond lengths** | | | | | | | | | | | |
| T1-O11 | 1.636(2) | 1.636(2) | 1.644(2) | 1.635(2) | 1.641(4) | 1.639(2) | 1.642(2) | 1.635(1) | 1.635(2) | 1.642(2) | 1.638(2) |
| T1-O21 | 1.642(2) | 1.638(2) | 1.637(2) | 1.643(2) | 1.661(4) | 1.642(2) | 1.638(2) | 1.640(1) | 1.641(2) | 1.646(2) | 1.647(2) |
| T1-O22 | 1.642(2) | 1.638(2) | 1.639(2) | 1.644(2) | 1.642(4) | 1.643(1) | 1.644(2) | 1.643(1) | 1.644(2) | 1.643(2) | 1.646(2) |
| T1-O31 | 1.637(2) | 1.645(2) | 1.641(2) | 1.650(2) | 1.644(3) | 1.644(1) | 1.650(2) | 1.646(1) | 1.645(2) | 1.646(2) | 1.647(2) |
| ⟨T1-O⟩ | 1.639 | 1.639 | 1.640 | 1.643 | 1.647 | 1.642 | 1.644 | 1.641 | 1.641 | 1.644 | 1.644 |
| T2-O11 | 1.635(2) | 1.639(2) | 1.635(2) | 1.640(2) | 1.635(4) | 1.634(2) | 1.633(2) | 1.637(1) | 1.639(2) | 1.636(2) | 1.643(2) |
| T2-O21 | 1.649(2) | 1.648(2) | 1.654(2) | 1.644(2) | 1.636(4) | 1.647(2) | 1.653(2) | 1.648(1) | 1.646(2) | 1.642(2) | 1.650(2) |
| T2-O22 | 1.641(2) | 1.640(2) | 1.640(2) | 1.643(2) | 1.644(4) | 1.640(2) | 1.643(2) | 1.639(1) | 1.642(2) | 1.639(2) | 1.645(2) |
| T2-O32 | 1.635(2) | 1.642(2) | 1.639(2) | 1.647(2) | 1.650(3) | 1.646(1) | 1.650(2) | 1.645(1) | 1.646(2) | 1.643(2) | 1.648(2) |
| ⟨T2-O⟩ | 1.640 | 1.642 | 1.642 | 1.644 | 1.641 | 1.642 | 1.645 | 1.642 | 1.643 | 1.640 | 1.646 |
| **Octahedral bond lengths** | | | | | | | | | | | |
| M2-O31 | 1.949(2) | 1.917(2) | 1.927(2) | 1.926(2) | 1.942(4) | 1.926(1) | 1.921(2) | 1.923(1) | 1.924(2) | 1.923(2) | 1.925(2) |
| M2-O31′ | 1.970(2) | 1.944(2) | 1.942(2) | 1.944(2) | 1.959(4) | 1.947(1) | 1.940(2) | 1.950(1) | 1.946(2) | 1.947(2) | 1.952(2) |
| M2-O32 | 1.970(2) | 1.940(2) | 1.943(2) | 1.945(2) | 1.942(4) | 1.945(1) | 1.943(2) | 1.947(1) | 1.945(2) | 1.951(2) | 1.951(2) |
| M2-O32′ | 1.949(2) | 1.920(2) | 1.928(2) | 1.923(2) | 1.940(4) | 1.925(1) | 1.920(2) | 1.924(1) | 1.918(2) | 1.920(2) | 1.925(2) |
| M2-O4 | 1.939(2) | 1.908(2) | 1.912(2) | 1.908(2) | 1.930(4) | 1.911(2) | 1.913(2) | 1.906(1) | 1.911(2) | 1.913(2) | 1.915(2) |
| M2-O4′ | 1.941(2) | 1.910(2) | 1.916(2) | 1.920(2) | 1.932(4) | 1.911(1) | 1.914(2) | 1.909(1) | 1.912(2) | 1.913(2) | 1.916(2) |
| ⟨M2-O⟩ | 1.953 | 1.923 | 1.928 | 1.928 | 1.941 | 1.927 | 1.925 | 1.927 | 1.926 | 1.928 | 1.931 |
| M1-O31 (×2) | 2.248(2) | 2.263(2) | 2.263(2) | 2.274(2) | 2.252(4) | 2.265(1) | 2.273(2) | 2.268(1) | 2.267(2) | 2.266(2) | 2.276(2) |
| M1-O32 (×2) | 2.251(2) | 2.274(2) | 2.270(2) | 2.267(2) | 2.271(4) | 2.267(1) | 2.271(2) | 2.270(1) | 2.271(2) | 2.269(2) | 2.276(2) |
| M1-O4 (×2) | 2.191(2) | 2.192(2) | 2.192(2) | 2.191(2) | 2.188(4) | 2.196(1) | 2.197(2) | 2.198(1) | 2.196(2) | 2.196(2) | 2.200(2) |
| ⟨M1-O⟩ | 2.230 | 2.243 | 2.241 | 2.244 | 2.237 | 2.243 | 2.247 | 2.246 | 2.245 | 2.244 | 2.250 |
| **Interlayer cation bond lengths** | | | | | | | | | | | |
| A-O11 (×2) | 2.966(2) | 2.868(2) | 2.870(2) | 2.883(3) | 2.904(4) | 2.879(2) | 2.878(2) | 2.884(1) | 2.874(2) | 2.881(2) | 2.888(2) |
| A-O11′ (×2) | 3.396(2) | 3.499(2) | 3.506(3) | 3.514(3) | 3.478(4) | 3.504(2) | 3.518(2) | 3.493(1) | 3.513(2) | 3.501(2) | 3.505(2) |
| A-O21 (×2) | 2.932(2) | 2.843(2) | 2.847(2) | 2.860(3) | 2.885(4) | 2.855(2) | 2.851(2) | 2.860(1) | 2.853(2) | 2.859(2) | 2.862(2) |
| A-O21′ (×2) | 3.230(2) | 3.267(2) | 3.272(2) | 3.278(3) | 3.253(4) | 3.272(2) | 3.280(2) | 3.266(1) | 3.274(2) | 3.269(2) | 3.275(2) |
| A-O22 (×2) | 2.931(2) | 2.836(2) | 2.845(2) | 2.848(2) | 2.872(4) | 2.846(1) | 2.844(2) | 2.850(1) | 2.843(2) | 2.850(2) | 2.854(2) |
| A-O22′ (×2) | 3.234(2) | 3.288(2) | 3.283(2) | 3.294(2) | 3.278(4) | 3.286(2) | 3.294(2) | 3.282(1) | 3.287(2) | 3.289(2) | 3.287(2) |
| A-O4 (×2) | 3.982(2) | 3.993(2) | 3.999(2) | 4.007(2) | 4.001(4) | 3.997(1) | 4.010(2) | 3.998(1) | 3.998(2) | 3.998(2) | 4.005(2) |
| $\langle A\text{-}O\rangle_{inner}$ | 2.943 | 2.849 | 2.854 | 2.864 | 2.887 | 2.860 | 2.858 | 2.865 | 2.857 | 2.863 | 2.868 |
| $\langle A\text{-}O\rangle_{outer}$ | 3.287 | 3.351 | 3.353 | 3.362 | 3.336 | 3.354 | 3.364 | 3.347 | 3.358 | 3.353 | 3.356 |
| Δ⟨A-O⟩ | 0.344 | 0.502 | 0.499 | 0.498 | 0.449 | 0.494 | 0.506 | 0.482 | 0.501 | 0.490 | 0.488 |

lated to thermal or displacement factors or to the partial covalent nature of the bonds affecting those atoms. Thus, only for crystals GA1, GFS15Ab, CC1b, C3-29b, B1b, C6Bb, and C3-31b could the peak suggest a plausible H location in view of the expected H position and the $R_{obs}$ value obtained. No attempts were made to introduce the coordinates of the H in each refinement.

Crystallographic coordinates and isotropic and anisotropic temperature factors are reported in Table 2 and relevant bond lengths are listed in Table 3. Observed and calculated structure factors are listed in Table 4[1]. The refined site-scattering values in electrons per formula unit (epfu), as estimated by structure refinement and electron microprobe analysis (EPMA), are given and compared in Table 5. Selected parameters derived from structure refinements are reported in Table 6.

### Chemical analyses

The chemical data were obtained by combining the results of: (1) wavelength-dispersive electron microprobe analyses (mean of 6–10 analytical points) on the same crystals used for the structure refinement (ARL-SEMQ microprobe operating at conditions: 15 KV accelerating voltage and 15 nA sample current, with a beam diameter of about 3 μm); (2) $Fe^{2+}$ and $(OH)^-$ determination on several crystals from the same rock sample that yielded the crystals used for the structure refinement. The weight loss was determined in argon gas to minimize the reaction $2FeO+2(OH)^- \rightarrow Fe_2O_3+H_2+O^{2-}$ using a Seiko SSC 5200 thermal analyzer (heating rate 10 °C/min and flow rate 200 mL/min). The determination was based on the weight loss observed in the temperature range 450–1000 °C and adjusted according to the mean F content determined by microprobe analysis. The $Fe^{2+}$ was determined using the semi-microvolumetric method (Meyrowitz 1970). Oxide percentages and structural formulas based on $O_{12-x-y}(OH)_x F_y$ are reported in Table 5.

## CRYSTAL STRUCTURE AND CHEMISTRY

### General considerations

Compared with the composition of end-member muscovite, the crystals examined show octahedral substitution due to Mg and Fe, with small amounts of Mn and Ti present as well (Table 5). Figure 1a indicates that the samples studied agree most closely with the exchange vector $^{[6]}Al^{3+}_{-1}{}^{[4]}Al^{3+}_{-1}{}^{[6]}(Mg^{2+}, Fe^{2+})^{[4]}Si^{4+}$.

Because of the vacant octahedral M1 site, and given the larger lateral dimension of the tetrahedral sheet compared with the octahedral sheet, the 2:1 layer of an end-

[1] For a copy of Table 4, deposit item AM-98-012, contact the Business Office of the Mineralogical Society of America (see inside front cover of recent issue) for price information. Deposit items may also be available on the *American Mineralogist* web site at http://www.minsocam.org.

**TABLE 5.** Averaged chemical composition, structural formulas, mean atomic number of octahedral and interlayer sites from X-ray refinement, and electron microprobe analyses of muscovite-2*M*$_1$ crystals

| wt% | GA1 | RA1 | A4b | GFS15A | H87b | CC1b | C3-29b | B1b | C6Cb | C6Bb | C3-31b |
|---|---|---|---|---|---|---|---|---|---|---|---|
| $SiO_2$ | 47.89 | 47.45 | 43.66 | 45.45 | 45.40 | 47.58 | 45.80 | 45.93 | 46.84 | 42.54 | 47.49 |
| $TiO_2$ | 0.12 | 0.79 | 0.38 | 0.48 | 0.04 | 1.27 | 0.67 | 1.23 | 0.79 | 1.02 | 0.43 |
| $Al_2O_3$ | 28.98 | 32.98 | 37.39 | 35.99 | 32.59 | 33.60 | 35.56 | 34.58 | 32.83 | 36.80 | 31.20 |
| $Fe_2O_3$ | — | — | 1.75 | 0.21 | 3.11 | — | — | — | — | — | 1.61 |
| FeO | 5.03 | 2.18 | — | 1.00 | 2.35 | 1.29 | 1.23 | 1.24 | 2.25 | 1.21 | 1.50 |
| MgO | b.d.t | 0.65 | 0.51 | 0.69 | b.d.t | 0.67 | 0.55 | 0.70 | 1.53 | 1.49 | 1.59 |
| MnO | 1.28 | 0.05 | 0.01 | b.d.t | 0.14 | 0.02 | 0.08 | b.d.t | 0.06 | 0.02 | 0.01 |
| CaO | b.d.t | b.d.t | b.d.t | b.d.t | b.d.t | b.d.t | 0.77 | b.d.t | b.d.t | 0.05 | 0.10 |
| BaO | 0.41 | b.d.t | 0.09 | b.d.t | b.d.t | 0.01 | b.d.t | 0.08 | 0.04 | b.d.t | 0.15 |
| $Na_2O$ | 0.10 | 0.66 | 0.70 | 0.65 | 0.41 | 0.65 | 0.45 | 0.54 | 0.68 | 0.42 | 0.38 |
| $K_2O$ | 11.31 | 10.74 | 10.76 | 10.79 | 11.05 | 10.91 | 10.32 | 10.95 | 10.63 | 10.79 | 10.91 |
| $H_2O$ | 3.85 | 4.14 | 4.20 | 4.30 | 3.90 | 4.01 | 3.66 | 3.68 | 3.47 | 3.74 | 4.63 |
| F | 1.01 | 0.35 | 0.54 | 0.44 | 1.00 | b.d.t | 0.91 | 1.07 | 0.88 | 1.91 | b.d.t |
| Sum | 99.98 | 99.99 | 99.99 | 100 | 99.99 | 100.01 | 100.00 | 100.00 | 100.00 | 99.99 | 100.00 |
| **Formula proportions (apfu) based on $O_{(12-x-y)}(OH)_xF_y$** | | | | | | | | | | | |
| Si | 3.30 | 3.18 | 2.92 | 3.03 | 3.09 | 3.18 | 3.07 | 3.09 | 3.17 | 2.87 | 3.18 |
| Al | 0.70 | 0.82 | 1.08 | 0.97 | 0.91 | 0.82 | 0.93 | 0.91 | 0.83 | 1.13 | 0.82 |
| Sum | 4.00 | 4.00 | 4.00 | 4.00 | 4.00 | 4.00 | 4.00 | 4.00 | 4.00 | 4.00 | 4.00 |
| Ti | 0.01 | 0.04 | 0.02 | 0.02 | — | 0.06 | 0.03 | 0.06 | 0.04 | 0.05 | 0.02 |
| $Fe^{3+}$ | — | — | 0.09 | 0.01 | 0.16 | — | — | — | — | — | 0.08 |
| $Fe^{2+}$ | 0.29 | 0.12 | — | 0.06 | 0.13 | 0.07 | 0.07 | 0.07 | 0.13 | 0.07 | 0.08 |
| Mg | — | 0.06 | 0.05 | 0.07 | — | 0.07 | 0.06 | 0.07 | 0.15 | 0.15 | 0.16 |
| Mn | 0.07 | — | — | — | 0.01 | — | — | — | — | — | — |
| Al | 1.65 | 1.78 | 1.88 | 1.86 | 1.71 | 1.83 | 1.88 | 1.83 | 1.78 | 1.80 | 1.64 |
| Sum | 2.02 | 2.00 | 2.04 | 2.02 | 2.01 | 2.03 | 2.04 | 2.03 | 2.10 | 2.07 | 1.98 |
| Na | 0.01 | 0.09 | 0.09 | 0.08 | 0.05 | 0.08 | 0.06 | 0.07 | 0.09 | 0.05 | 0.05 |
| K | 0.99 | 0.92 | 0.92 | 0.92 | 0.96 | 0.93 | 0.88 | 0.94 | 0.92 | 0.93 | 0.93 |
| Ca | — | — | — | — | — | — | 0.06 | — | — | — | 0.01 |
| Ba | 0.01 | — | — | — | — | — | — | — | — | — | — |
| Sum | 1.01 | 1.01 | 1.01 | 1.00 | 1.01 | 1.01 | 1.00 | 1.01 | 1.01 | 0.98 | 0.94 |
| OH | 1.77 | 1.85 | 1.88 | 1.91 | 1.77 | 1.79 | 1.64 | 1.65 | 1.56 | 1.68 | 2.07 |
| F | 0.22 | 0.07 | 0.11 | 0.09 | 0.22 | — | 0.19 | 0.23 | 0.19 | 0.41 | — |
| O | 10.01 | 10.08 | 10.01 | 10.00 | 10.01 | 10.21 | 10.17 | 10.12 | 10.25 | 9.91 | 9.93 |
| Sum | 12.00 | 12.00 | 12.00 | 12.00 | 12.00 | 12.00 | 12.00 | 12.00 | 12.00 | 12.00 | 12.00 |
| **Mean atomic number ($e^-$)** | | | | | | | | | | | |
| M1(Xref) | 0.64(4) | 0.97(4) | 0.46(5) | 0.44(5) | 0.84(6) | 0.32(3) | 0.49(6) | 0.38(4) | 1.73(8) | 0.88(8) | 0.39(4) |
| M2(Xref) | 15.5(2) | 13.9(2) | 13.5(2) | 13.7(2) | 15.0(3) | 13.8(1) | 13.7(2) | 13.7(1) | 14.0(2) | 13.6(2) | 13.8(2) |
| $M1+M2_{Xref}$ | 31.7(4) | 28.2(4) | 27.5(4) | 27.8(4) | 30.8(7) | 27.9(3) | 27.8(4) | 27.8(3) | 29.8(4) | 28.2(4) | 28.1(4) |
| $M1+M2_{EPMA}$ | 31.0 | 27.9 | 27.8 | 27.3 | 30.0 | 27.8 | 27.6 | 27.8 | 29.2 | 28.1 | 27.8 |
| A(Xref) | 19.82(5) | 18.22(5) | 18.41(6) | 18.20(6) | 18.81(9) | 18.70(4) | 18.68(5) | 18.70(4) | 18.54(6) | 18.26(5) | 18.73(6) |
| A(EPMA) | 19.48 | 18.47 | 18.47 | 18.36 | 18.79 | 18.55 | 18.58 | 18.63 | 18.47 | 18.22 | 18.42 |

*Note:* Xref = X-ray refinement; EPMA = electron microprobe; b.d.t = below detection threshold; standard deviations in parentheses.

member muscovite is normally distorted, with, for example, a significant tetrahedral rotation angle or markedly flattened octahedra. Where a larger cation, such as $Fe^{2+}$, $Fe^{3+}$, and Mg, substitutes for Al, the octahedral sheet increases in size and more closely matches the dimensions of the tetrahedral sheet, thereby reducing distortion. In this way, as suggested by Guidotti et al. (1989, 1992), octahedral substitution causes an increase in the *a* and *b* cell parameters and, as a consequence, an enlargement in cell volume (Fig. 1b). Substitution of Na [$0.01 \leq Na \leq 0.09$ atoms per formula unit (apfu)] for K also influences cell volume: as Na increases, the cell becomes smaller because *a*, *b*, and *c* all decrease. Sample GA1, with 18.3% octahedral substitution (calculated as a ratio between the sum of octahedral components without and with octahedral Al) and with a small amount of Na, displays the greatest volume.

In dioctahedral micas, the position of H is expected to be at a distance of 0.928 Å from O; the O-H vector, inclined from the (001) plane by about 12°, points generally in the direction of the O11 basal anion (Rothbauer 1971; Guggenheim et al. 1987). Small positive DED anomalies (see Experimental details section) were located near the O4 atom at a distance consistent with an O-H bond. The calculated polar angle (ρ) values are close to the expected value of +12° for crystals CC1b, C3-29b, B1b, and C6Bb, whereas for crystals GA1, GFS15Ab, and C3-31b the values are −6.9°, 6.0°, and 26.8°, respectively. Bookin and Drits (1982) suggested that the O-H vector orientation is strongly affected by: (1) the distortion of polyhedra; (2) the localization of uncompensated charge in 2:1 layer; (3) the mean charges of M1 and A sites; and (4) the degree and mode of cation ordering. Therefore, the variation of ρ may be considered an indication of phengitic substitution. As suggested by Rule and Bailey (1985), negative values of ρ (i.e., the O-H vector points within the M1 site) could be due to the need to counterbalance the repulsion of the highly charged tetrahedral cations (e.g., sample GA1 has the greatest Si content and ρ = −6.9°), whereas the charge and electron density at

**TABLE 6.** Selected tetrahedral, octahedral, and interlayer parameters derived from structure refinements of muscovite-2$M_1$ crystals

| | GA1 | RA1 | A4b | GFS15Ab | H87b | CC1b | C3-29b | B1b | C6Cb | C6Bb | C3-31b |
|---|---|---|---|---|---|---|---|---|---|---|---|
| **Tetrahedral parameters** | | | | | | | | | | | |
| $\alpha$ (°) | 7.70 | 11.29 | 11.22 | 11.19 | 10.05 | 11.10 | 11.38 | 10.84 | 11.26 | 11.01 | 10.94 |
| $\Delta z$ (Å) | 0.1796 | 0.2235 | 0.2232 | 0.2235 | 0.2156 | 0.2216 | 0.2296 | 0.2197 | 0.2252 | 0.2200 | 0.2227 |
| $\tau_{T1}$ (°) | 111.5 | 111.1 | 111.1 | 110.8 | 111.1 | 111.0 | 111.0 | 111.1 | 110.9 | 111.0 | 111.1 |
| $\tau_{T2}$ (°) | 111.5 | 111.0 | 111.1 | 110.9 | 111.2 | 111.0 | 111.0 | 111.1 | 111.0 | 111.1 | 111.2 |
| $TAV_{T1}$ (°)$^2$ | 6.1 | 5.0 | 4.9 | 4.3 | 4.6 | 4.4 | 4.5 | 4.9 | 4.4 | 4.3 | 5.0 |
| $TAV_{T2}$ (°)$^2$ | 6.4 | 5.6 | 5.6 | 4.6 | 6.1 | 5.0 | 4.8 | 5.2 | 5.0 | 5.0 | 5.6 |
| $TQE_{T1}$ | 1.0015 | 1.0013 | 1.0013 | 1.0011 | 1.0012 | 1.0011 | 1.0012 | 1.0013 | 1.0011 | 1.0011 | 1.0013 |
| $TQE_{T2}$ | 1.0015 | 1.0014 | 1.0014 | 1.0012 | 1.0016 | 1.0013 | 1.0012 | 1.0013 | 1.0013 | 1.0013 | 1.0014 |
| $Volume_{T1}$ (Å)$^3$ | 2.256 | 2.256 | 2.261 | 2.272 | 2.289 | 2.268 | 2.275 | 2.264 | 2.266 | 2.277 | 2.278 |
| $Volume_{T2}$ (Å)$^3$ | 2.259 | 2.269 | 2.267 | 2.275 | 2.262 | 2.267 | 2.279 | 2.269 | 2.273 | 2.261 | 2.286 |
| $BLD_{T1}$ (%) | 0.166 | 0.276 | 0.133 | 0.245 | 0.423 | 0.110 | 0.192 | 0.218 | 0.212 | 0.103 | 0.189 |
| $BLD_{T2}$ (%) | 0.303 | 0.169 | 0.365 | 0.137 | 0.344 | 0.270 | 0.412 | 0.257 | 0.178 | 0.160 | 0.144 |
| $ELD_{T1}$ (%) | 1.243 | 1.188 | 1.110 | 1.071 | 1.106 | 1.024 | 1.111 | 1.134 | 1.060 | 1.072 | 1.096 |
| $ELD_{T2}$ (%) | 1.172 | 1.082 | 1.034 | 1.092 | 1.343 | 1.090 | 1.065 | 1.095 | 1.101 | 1.110 | 1.146 |
| **Octahedral parameters** | | | | | | | | | | | |
| $\psi_{M1}$ (°) | 61.82 | 62.26 | 62.14 | 62.30 | 62.02 | 62.23 | 62.29 | 62.26 | 62.28 | 62.25 | 62.25 |
| $\psi_{M2}$ (°) | 57.37 | 57.12 | 57.10 | 57.24 | 57.25 | 57.17 | 57.13 | 57.14 | 57.17 | 57.18 | 57.13 |
| $e_{s\,M1}$ (Å) | 2.881 | 2.881 | 2.884 | 2.881 | 2.883 | 2.882 | 2.885 | 2.885 | 2.882 | 2.883 | 2.891 |
| $e_{s\,M2}$ (Å) | 2.476 | 2.416 | 2.428 | 2.420 | 2.451 | 2.423 | 2.417 | 2.421 | 2.418 | 2.423 | 2.426 |
| $e_{u\,M1}$ (Å) | 3.405 | 3.439 | 3.433 | 3.442 | 3.422 | 3.437 | 3.446 | 3.443 | 3.442 | 3.440 | 3.450 |
| $e_{u\,M2}$ (Å) | 2.849 | 2.797 | 2.804 | 2.807 | 2.827 | 2.805 | 2.800 | 2.803 | 2.803 | 2.806 | 2.809 |
| $OQE_{M1}$ | 1.0329 | 1.0375 | 1.0363 | 1.0379 | 1.0350 | 1.0371 | 1.0378 | 1.0374 | 1.0377 | 1.0373 | 1.0374 |
| $OQE_{M2}$ | 1.0137 | 1.0167 | 1.0160 | 1.0167 | 1.0150 | 1.0164 | 1.0168 | 1.0166 | 1.0167 | 1.0164 | 1.0166 |
| $OAV_{M1}$ (°) | 99.6 | 111.7 | 108.3 | 112.6 | 104.7 | 110.6 | 112.3 | 111.5 | 112.3 | 111.2 | 111.3 |
| $OAV_{M2}$ (°) | 49.7 | 60.8 | 58.4 | 60.7 | 54.6 | 59.6 | 61.3 | 60.4 | 60.7 | 59.8 | 60.3 |
| $Volume_{M1}$ (Å) | 14.085 | 14.246 | 14.237 | 14.256 | 14.184 | 14.247 | 14.315 | 14.293 | 14.270 | 14.265 | 14.388 |
| $Volume_{M2}$ (Å) | 9.734 | 9.252 | 9.331 | 9.318 | 9.530 | 9.317 | 9.278 | 9.304 | 9.289 | 9.324 | 9.364 |
| $BLD_{M2}$ (%) | 0.580 | 0.657 | 0.500 | 0.584 | 0.357 | 0.638 | 0.573 | 0.766 | 0.677 | 0.728 | 0.717 |
| $ELD_{M1}$ (%) | 8.334 | 8.825 | 8.692 | 7.174 | 8.551 | 8.785 | 8.852 | 8.817 | 8.845 | 8.806 | 8.807 |
| $ELD_{M2}$ (%) | 5.200 | 6.683 | 5.527 | 5.657 | 5.392 | 5.602 | 6.550 | 5.630 | 5.651 | 5.617 | 5.622 |
| **Sheet thickness** | | | | | | | | | | | |
| Tetrahedral | 2.247 | 2.242 | 2.242 | 2.242 | 2.251 | 2.242 | 2.246 | 2.245 | 2.241 | 2.242 | 2.249 |
| Octahedral | 2.106 | 2.088 | 2.095 | 2.086 | 2.099 | 2.090 | 2.090 | 2.091 | 2.088 | 2.090 | 2.096 |
| Interlayer | 3.370 | 3.380 | 3.385 | 3.405 | 3.381 | 3.391 | 3.408 | 3.388 | 3.393 | 3.391 | 3.394 |
| $\Delta_{TM}$ (Å) | 0.592 | 0.568 | 0.563 | 0.576 | 0.538 | 0.566 | 0.574 | 0.556 | 0.573 | 0.564 | 0.559 |

*Note:* $\alpha$ (tetrahedral rotation angle) = $\Sigma_{i=1}^{6}\alpha_i/6$ where $\alpha_i = |120° - \phi_i|/2$ and where $\phi_i$ is the angle between basal edges of neighboring tetrahedra articulated in the ring. $\Delta z = [Z_{(O_{basal})max} - Z_{(O_{basal})min}][c\sin\beta]$. $\tau$ (tetrahedral flattening angle) = $\Sigma_{i=1}^{3}(O_{basal} - \hat{T} - O_{basal})_i/3$. TAV (tetrahedral angle variance = $\Sigma_{i=1}^{3}(\theta_i - 109.47)^2/5$ (Robinson et al. 1971). TQE (tetrahedral quadratic elongation) = $\Sigma_{i=1}^{4}(l_i/l_o)^2/4$ where $l_o$ is the center to vertex distance for an undistorted tetrahedron whose volume is equal to that of the distorted tetrahedron with bond length $l_i$ (Robinson et al. 1971). $\psi$ (octahedral flattening angle) = $\cos^{-1}$[octahedral thickness/(2⟨M-O⟩)] (Donnay et al. 1964). $e_u$, $e_s$ = mean lengths of unshared and shared edges, respectively (Toraya 1981). OQE (octahedral quadratic elongation) $\Sigma_{i=1}^{6}(l_i/l_o)^2/6$ where $l_o$ is the center to vertex distance for an undistorted octahedron whose volume is equal to that of the distorted octahedron with bond length $l_i$ (Robinson et al. 1971). OAV (octahedral angle variance) = $\Sigma_{i=1}^{12}(\theta_i - 90°)^2/11$ (Robinson et al. 1971). BLD = (bond length distortion)$(100/n)\Sigma_{i=1}^{n}$ [|$(X - O)_i - (\langle X - O\rangle)$|]/$(\langle X - O\rangle)$% where $n$ is the number of bonds and $(X - O)$ the central cation-oxygen length (Renner and Lehmann 1986). ELD = (edge length distortion) $(100/n)\Sigma_{i=1}^{n}$ [|$(O - O)_i - (\langle O - O\rangle)$|]/$(\langle O - O\rangle)$% where $n$ is the number of bonds and $(O - O)$ the polyhedron edge length (Renner and Lehmann 1986). $\Delta_{TM}$ (dimensional misfit) = $2\sqrt{3}\langle O - O\rangle_{basal} - 3\sqrt{2}\,(2\langle M2 - O\rangle + \langle M1 - O\rangle)/3$ (Toraya 1981).

the M2 and A sites coupled with the partial M1 occupancy could repel the proton away from the (001) plane.

### Tetrahedral sheet

The tetrahedral sheet composition of the studied specimens ranges from 0.70 apfu $\leq$ Al $\leq$ 1.13 apfu: the low Al value is found in sample GA1, the high one in C6Bb. This variation in Al content about the ideal Si:Al = 3:1 ratio could be due to both the $^{[6]}Al^{3+}_{-1}{}^{[4]}Al^{3+}_{-1}{}^{[6]}(Mg^{2+}, Fe^{2+})^{[4]}Si^{4+}$ and the $^{[6]}Al^{3+}_{-1}{}^{[4]}Si^{4+}_{-1}{}^{[6]}Ti^{4+}{}^{[4]}Al^{3+}$ exchange operators. The first exchange vector involves the substitution of a larger cation for Al in octahedra and substitution of smaller Si for Al in tetrahedra. As the Si content increases, the tetrahedral sheet becomes thinner and a reduction in lateral size occurs (Fig. 2a), thereby decreasing the volume of tetrahedra. Simultaneously, the octahedral sheet increases laterally and vertically; the fit between the octahedral and tetrahedral sheets improves and fewer distortions from hexagonal symmetry ($\alpha$ value) are required by the tetrahedral ring (Fig. 2b). Also, $\Delta z$, the corrugation of the basal O atoms due to tetrahedral tilting around the vacant site, is less marked. The low $\Delta z$ values appear in crystals with the greatest octahedral substitution. According to Lee and Guggenheim (1981), the improved coplanarity of the basal O atoms may be attributed to the increase in octahedral substitution, which reduces differences in the M1 and M2 site volumes (Table 3) and requires less tetrahedral tilting to fit O31 and O32 O atoms. The direct relationship between $\alpha$ and $\Delta z$ confirms this trend (Fig. 2c).

There are no measurable differences between T1 and T2 and thus they are equivalent with respect to Al,Si oc-

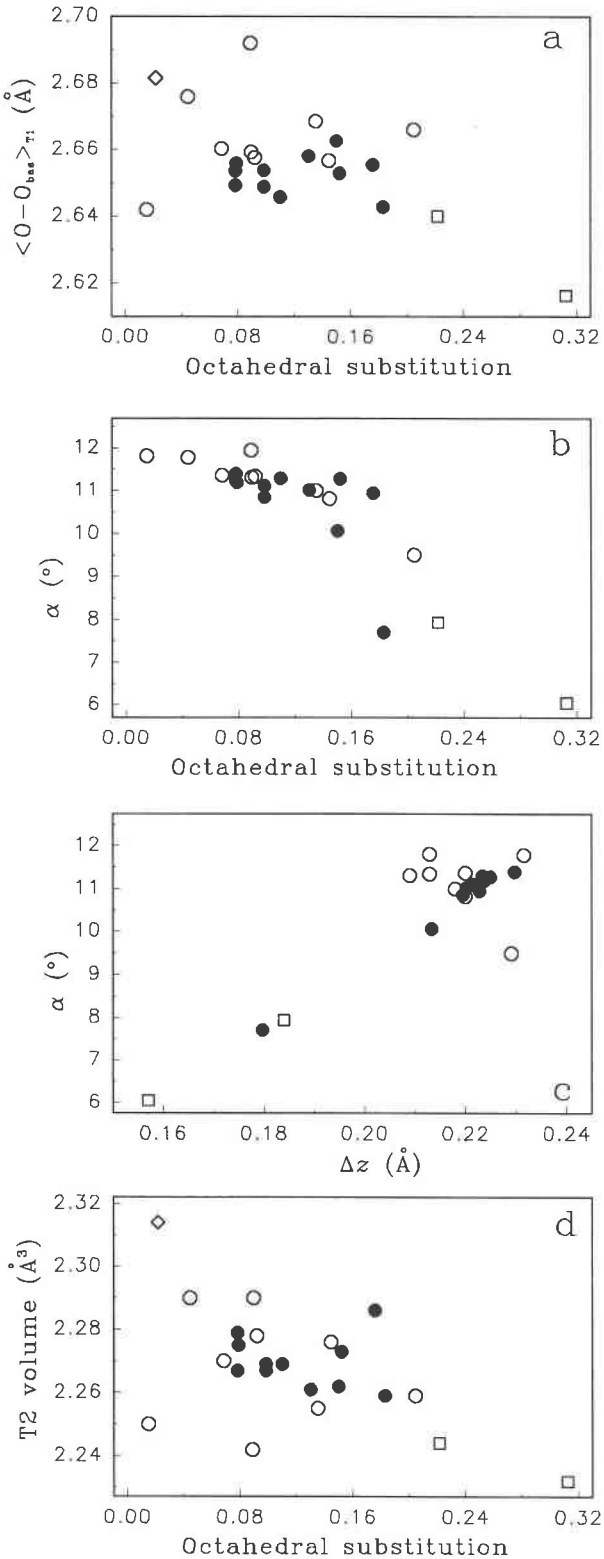


**FIGURE 2.** (**a**) <O-O$_{bas}$>$_{T1}$ (Å) vs. octahedral substitution; (**b**) tetrahedral ring distortion (α°) vs. octahedral substitution; (**c**) α (°) vs. corrugation of basal O atoms Δz (Å); and (**d**) T2 tetrahedral volume (Å$^3$) vs. octahedral substitution of muscovite-2$M_1$ crystals. The octahedral substitution is calculated as in Figure 1. Symbols: filled circles = samples from this study; open circles = muscovite samples from literature (Birle and Tettenhorst 1968; Güven 1971; Rothbauer 1971; Richardson and Richardson 1982; Knurr and Bailey 1986; Guggenheim et al. 1987; Catti et al. 1989, 1994); open squares = phengites from literature (Güven 1971; Rule and Bailey 1985); open diamond = paragonite from Lin and Bailey (1984).
←

cupancy (Table 3). Also, the ratio between the T1 and T2 volumes is constant for all specimens. The volumes crudely decrease, thus increasing phengitic substitution in the same way for both T1 and T2 (Fig. 2d).

### Octahedral sheet

As in most muscovite crystals, the vacancy in the studied samples is ordered in the trans-M1 site; no other ordering in M2 sites is found. The mean electron count for the M2 site is always greater than 13 e$^-$, indicating that elements heavier than Al occupy the octahedral sheet, which is consistent with the chemical composition. Furthermore, a small excess of electron density is found in the M1 site, indicating partial occupancy. In muscovite, because the M1 site is essentially vacant, the M2 site is distorted due to repulsion between the adjacent highly charged Al cations; edges shared between occupied octahedra are shorter than unshared edges (Bailey 1984). As the octahedral substitution increases, the octahedral <M2-O> distance extends (Fig. 3a) and the site is less distorted (Table 6). Thus, the larger cations impinge upon and reduce the M1 site size, tetrahedra tilt less out-of-plane to fit the lateral edge of the vacant site, and the differences in both shape and distortion parameters between the two octahedra progressively decrease. The flattening of octahedra is strictly related to the amount of octahedral substitution and, accordingly, to the interlayer cavity formed (Figs. 3b and 3c).

### Interlayer cations

Because the interlayer composition of the samples studied is not affected by significant substitution (only a small amount of Na), the geometry of the A site reflects the layer chemistry. The sixfold-coordination with the basal inner O is distorted and elongated parallel to **c*** (Table 3). The largest A-O distance is A-O11, compared with other inner distances (A-O21 and A-O22). This large A-O11 distance is attributed to the corrugation of the basal O plane, to the unequal shape and dimensions of M1 vs. M2, and to the orientation of the O-H vector, which generally points to the O11 anion thus weakening the A-O11 bond strength (Guggenheim at al. 1987). The A-O11 distance varies according to A-O21 and A-O22 inner distances as a consequence of the tetrahedral and octahedral

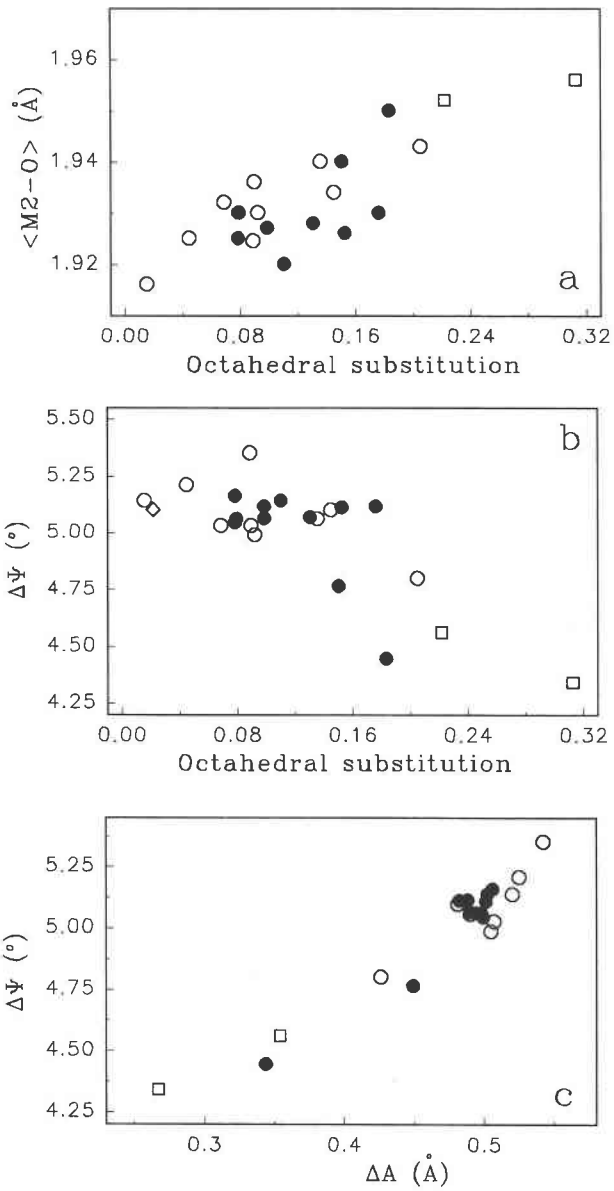


**FIGURE 3.** (**a**) <M2-O> (Å) vs. octahedral substitution; (**b**) difference between the flattening of the two octahedral cavities $\Delta\Psi(°)$ ($\Delta\Psi = \Psi_{M1} - \Psi_{M2}$) vs. octahedral substitution; (**c**) $\Delta\Psi(°)$ vs. difference between outer and inner interlayer cation coordination $\Delta A$ (Å) ($\Delta A = <A\text{-}O>_{outer} - <A\text{-}O>_{inner}$) of muscovite-$2M_1$ crystals. The octahedral substitution is calculated as in Figure 1. Symbols as defined in Figure 2.

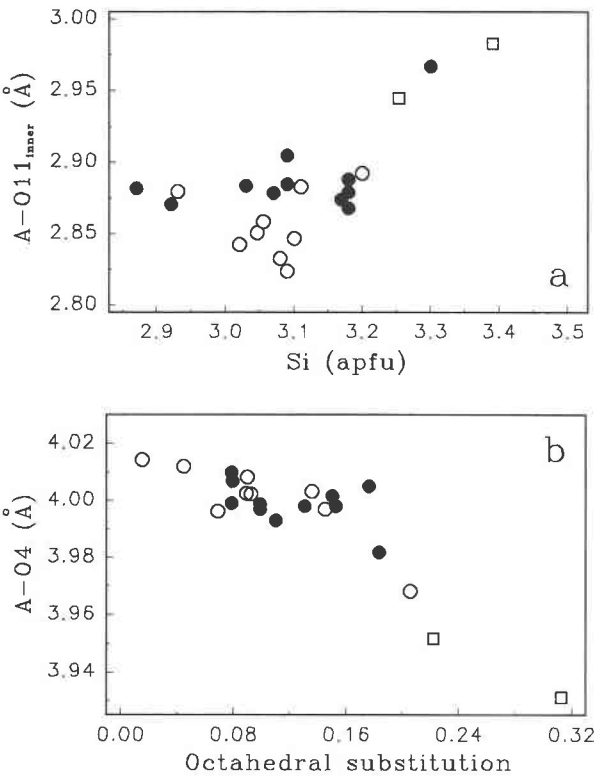


**FIGURE 4.** (**a**) A-O11$_{inner}$ distance (Å) vs. Si content (apfu); (**b**) A-O4 distance (Å) vs. octahedral substitution (calculated as in Fig. 1) of muscovite-$2M_1$ crystals. Symbols as defined in Figure 1.

phengitic substitution (Fig. 4a). As inner distances around the interlayer cation increases because of tetrahedral rotation, the difference between outer and inner coordination decrease. A consequence of the decrease in the $\alpha$ value is an increase in the size of the interlayer site, which allows the cation to become embedded more deeply in the ring. The A-O4 distance is a measure of how deeply the A cation enters the cavity and is mainly influenced by octahedral substitution (Fig. 4b). Interlayer separation is related to the location of the A cation in the interlayer cavity.

## ACKNOWLEDGMENTS

We are grateful to S. Guggenheim for his constructive criticism of the first draft of the manuscript and acknowledge the comments of an anonymous reviewer who led us to reconsider some of our original conclusions. We also wish to thank F.P. Sassi for helpful discussion. We are indebted to C. Ghezzo, A. Rossi, and A. Gamboni for provision of the specimens studied. This research was supported by Ministero dell'Università e della Ricerca Scientifica e Tecnologica (MURST) and CNR of Italy. We are also grateful to CNR and to CIGS (University of Modena) for the use of microprobe and single-crystal X-ray diffractometers.

## REFERENCES CITED

Amisano-Canesi, A., Chiari, G., Ferraris, G., Ivaldi, G., and Soboleva, S.V. (1994) Muscovite- and phengite-3*T*: crystal structure and conditions of formation. European Journal of Mineralogy, 6, 489–496.

Bailey, S.W. (1984) Crystal chemistry of the true micas. In Mineralogical Society of America Reviews in Mineralogy, 13, 13–60.

Birle, J.D. and Tettenhorst, R. (1968) Refined muscovite structure. Mineralogical Magazine, 36, 883–886.

Bookin, A.S. and Drits, V.A. (1982) Factor affecting orientation of O-H-vector in micas. Clays and Clay Minerals, 30, 415–421.

Busing, W.R., Martin, K.O., and Levi, H.S. (1962) ORFLS, a Fortran crystallographic least-squares program. U.S. National Technical Information Section, ORNL-TM-305.

Catti, M., Ferraris, G., and Ivaldi, G. (1989) Thermal strain analysis in

the crystal structure of muscovite at 700 °C. European Journal of Mineralogy, 1, 625–632.

Catti, M., Ferraris, G., Hull, S., and Pavese A. (1994) Powder neutron diffraction study of $2M_1$ muscovite at room pressure and at 2 GPa. European Journal of Mineralogy, 6, 171–178.

Comodi, P. and Zanazzi, P.F. (1995) High-pressure structural study of muscovite. Physics and Chemistry of Minerals, 22, 170–177.

Donnay, G., Morimoto, N., Takeda, H., and Donnay, D.H. (1964) Trioctahedral one-layer micas: 1. Crystal structure of a synthetic iron mica. Acta Crystallographica, 17, 1369–1373.

Guggenheim, S., Chang, Y.H., and Koster van Groos, A.F. (1987) Muscovite dehydroxylation: High-temperature studies. American Mineralogist, 72, 537–550.

Guidotti, C.V. (1978) Compositional variation of muscovite in medium- to high-grade metapelites of northwestern Maine. American Mineralogist, 63, 878–884.

——— (1984) Micas in metamorphic rocks. In Mineralogical Society of America Reviews in Mineralogy, 13, 357–468.

Guidotti, C.V. and Sassi, F.P. (1976) Muscovite as a petrogenetic indicator mineral in pelitic schist. Neues Jahrbuch fur Minerallogie Abhandlungen,127, 97–142.

Guidotti, C.V., Sassi, F.P., and Blencoe, J.G. (1989) Compositional controls on the $a$ and $b$ cell dimentions of $2M_1$ muscovite. European Journal of Mineralogy, 1, 71–84.

Guidotti, C.V., Mazzoli, C., Sassi, F.P., and Blencoe, J.G. (1992) Compositional controls on the cell dimentions of $2M_1$ muscovite and paragonite. European Journal of Mineralogy, 4, 283–297.

Guidotti, C.V., Sassi, F.P., Blencoe, J.G., and Selverstone, J. (1994a) The paragonite-muscovite solvus: I. P-T-X limits derived from the Na-K compositions of natural, quasibinary paragonite-muscovite pairs. Geochimica et Cosmochimica Acta, 58, 2269–2275.

Guidotti, C.V., Yates, M.G., Dyar, M.D., and Taylor, M.E. (1994b) Petrogenetic implications of the $Fe^{3+}$ content of muscovite in pelitic schists. American Mineralogist, 79, 793–795.

Güven, N. (1971) The crystal structures of $2M_1$ phengite and $2M_1$ muscovite. Zeitschrift für Kristallographie, 134, 196–212.

Güven, N. and Burnham, C.W. (1967) The crystal structure of $3T$ muscovite. Zeitschrift für Kristallographie, 125, 163–183.

Jackson, W.W. and West, J. (1930) The crystal structure of muscovite—$KAl_2(AlSi_3)O_{10}(OH)_2$. Zeitschrift für Kristallographie, 76, 211–227.

Jackson, W.W. and West, J. (1933) The crystal structure of muscovite—$KAl_2(AlSi_3)O_{10}(OH)_2$. Zeitschrift für Kristallographie, 85, 160–164.

Knurr, R.A. and Bailey, S.W. (1986) Refinement of Mn-substituted muscovite and phlogopite. Clays and Clay Minerals, 34, 7–16.

Lee, J.H. and Guggenheim, S. (1981) Single crystal X-ray refinement of pyrophyllite-1$Tc$. American Mineralogist, 66, 350–367.

Lin, C.Y. and Bailey, S.W. (1984) The crystal structure of paragonite-$2M_1$. American Mineralogist, 69, 122–127.

Meyrowitz, R. (1970) New semimicroprocedure for determination of ferrous iron in refractory silicate minerals using a sodium metafluoroborate decomposition. Analytical Chemistry, 42, 1110–1113.

Nelson, D.O. and Guggenheim, S. (1993). Inferred limitations to the oxidation of Fe in chlorite: A high-temperature single-crystal X-ray study. American Mineralogist, 78, 1197–1207.

Pavese, A., Ferraris, G., Prencipe, M., and Ibberson, R. (1997) Cation site ordering in phengite $3T$ from the Dora-maira massif (western Alps): a variable-temperature neutron powder diffraction study. European Journal of Mineralogy, 9, 1183–1190.

Radoslovich, E.W. (1960) The structure of muscovite, $KAl_2(Si_3Al)O_{10}(OH)_2$. Acta Crystallographica, 13, 919–932.

Renner, B. and Lehmann, G. (1986) Correlation of angular and bond length distortion in $TO_4$ units in crystals. Zeitschrift für Kristallographie, 175, 43–59.

Richardson, S.M. and Richardson, J.W. Jr. (1982) Crystal structure of a pink muscovite from Archer's Post, Kenya: implications for reverse pleochroism in dioctahedral micas. American Mineralogist, 67, 69–75.

Robinson, K., Gibbs, G.V., and Ribbe, P.H. (1971) Quadratic elongation: a quantitative measure of distortion in coordination polyhedra. Science, 172, 567–570.

Rothbauer, Von R. (1971) Untersuchung eines $2M_1$-muskovits mit neutronenstrahlen. Neues Jahrbuch für Mineralogie Monatshefte, 143–154.

Rule, A.C. and Bailey, S.W. (1985) Refinement of the crystal structure of phengite-$2M_1$. Clays and Clay Minerals, 33, 403–409.

Sassi, F.P., Guidotti, C.V., Rieder, M., and De Pieri, R. (1994) On occurrence of metamorphic $2M_1$ phengites: some thoughts on polytypism and crystallization conditions of $3T$ phengites. European Journal of Mineralogy, 6, 151–160.

Sidorenko, O.V., Zvyagin, B.B., and Soboleva, S.V. (1977) The crystal structure of paragonite 1$M$. Soviet Physics Crystallography, 22, 291–293.

Siemens (1993) XSCANS System—Technical reference. Siemens analytical X-ray instruments.

Toraya, H. (1981) Distortions of octahedra and octahedral sheets in 1$M$ micas and the relation to their stability. Zeitschrift für Kristallographie, 157, 173–190.

Tsipurskii, S.I. and Drits, V.A. (1977) Effectivity of the electronic method of intensity measurement in structural investigation by electron diffraction. Izvestija Akademii Nauk SSSR, Serija fiziko-matematicheskaja, 41, 2263–2271 (in Russian).

Ungaretti, L. (1980) Recent developments in X-ray crystal diffractometry applied to the crystal chemical study of amphiboles. Godisnjac Iugoslavenskog Centraza Kristalograiju, 15, 29–65.

Ungaretti, L., Lombardo, B., Domeneghetti, M.C., and Rossi, G. (1983) Crystal chemical evolution of amphiboles from eclogitised rocks of the Sesia-Lanzo Zone, Italian western Alps. Bulletin de Minèralogie, 106, 645–672.

Zhoukhlistov, A.P., Zvyagin, B.B., Soboleva, S.V., and Fedotov, A.F. (1973) The crystal structure of the dioctahedral mica $2M_2$ determined by high voltage electron diffraction. Clays and Clay Minerals, 21, 465–470.

Manuscript received October 21, 1997
Manuscript accepted February 17, 1998
Paper handled by Gilberto Artioli